

Research Article

Open Access



Si(111) islands on β -phase Si(111) $\sqrt{3} \times \sqrt{3}R30^\circ$ -Bi

Paola De Padova^{1,2}, Mieczysław Jałochowski³, Amanda Generosi¹, Carlo Ottaviani¹, Claudio Quaresima¹, Barbara Paci¹, Bruno Olivieri⁴, Mariusz Krawiec³

¹ISM-Consiglio Nazionale delle Ricerche, Roma 00133, Italy.

²Laboratori Nazionali di Frascati-Istituto Nazionale di Fisica Nucleare, Frascati 00044, Italy.

³Institute of Physics, Maria Curie-Skłodowska University, Lublin 20-031, Poland.

⁴ISAC-Consiglio Nazionale delle Ricerche, Roma 00133, Italy.

Correspondence to: Dr. Paola De Padova, ISM-Consiglio Nazionale delle Ricerche, Via Fosso del Cavaliere, 100, Roma 00133, Italy. E-mail: Paola.DePadova@ism.cnr.it; Prof. Mariusz Krawiec, Institute of Physics, Maria Curie-Skłodowska University, pl. M. Curie-Skłodowskiej 1, Lublin 20-031, Poland. E-mail: mariusz.krawiec@umcs.pl

How to cite this article: De Padova P, Jałochowski M, Generosi A, Ottaviani C, Quaresima C, Paci B, Olivieri B, Krawiec M. Si(111) islands on β -phase Si(111) $\sqrt{3} \times \sqrt{3}R30^\circ$ -Bi. *Microstructures* 2024;4:2024019. <https://dx.doi.org/10.20517/microstructures.2023.74>

Received: 9 Nov 2023 **First Decision:** 7 Dec 2023 **Revised:** 19 Dec 2023 **Accepted:** 23 Jan 2024 **Published:** 10 Apr 2024

Academic Editor: Junhao Lin **Copy Editor:** Pei-Yun Wang **Production Editor:** Pei-Yun Wang

Abstract

β -phase $\sqrt{3} \times \sqrt{3}R30^\circ$ -bismuth (Bi) on silicon (Si)(111) 7×7 surface has been exploited as a template for growing Si films. Two-dimensional Si islands with $\sqrt{3} \times \sqrt{3}$ reconstruction, parallel to that of Si(111) $\sqrt{3} \times \sqrt{3}R30^\circ$ -Bi, have been resolved by means of scanning tunneling microscopy, grazing-incidence X-ray diffraction (XRD) and low electron energy diffraction. Auger electron spectroscopy and scanning tunneling spectroscopy gave interesting electronic features on two-dimensional Si islands, with the evidence of a reduced band gap to ~ 0.55 eV, related to the presence of the underneath Bi layer, and atomic structural properties typical of Si(111). These experimental findings fully confirm the recently reported calculation based on the first-principles density functional theory, on the prediction of Si(111) growth on top of β -phase $\sqrt{3} \times \sqrt{3}R30^\circ$ -Bi/Si(111) 7×7 reconstruction, shedding new light on silicon structures.

Keywords: Materials science, 2D Si(111) island growth, AES, LEED, STM, STS, GIXRD

INTRODUCTION

The study of bismuth (Bi), started in ancient times^[1], has stimulated research in surface science physics aimed at understanding the structural and electronic properties of the atomic arrangement of Bi atoms, both on theoretical modelling and experimental fronts, of the Bi interface formation with silicon (Si)(111) 7×7 ^[2-6].



© The Author(s) 2024. **Open Access** This article is licensed under a Creative Commons Attribution 4.0 International License (<https://creativecommons.org/licenses/by/4.0/>), which permits unrestricted use, sharing, adaptation, distribution and reproduction in any medium or format, for any purpose, even commercially, as long as you give appropriate credit to the original author(s) and the source, provide a link to the Creative Commons license, and indicate if changes were made.



Depending on the growth parameters, mainly substrate temperature and Bi coverage, the Bi atoms can arrange on Si(111) 7×7 in diverse structures, called α -phase, β -phase and honeycomb phase^[7-11]. The α -phase is obtained at a temperature of ~ 613 K, in addition to a Bi coverage of one-third monolayer (ML); β -phase manifests at a temperature of ~ 523 K and a coverage of one ML of Bi. As a matter of fact, in the interval of temperature $298 \text{ K} < T < 523 \text{ K}$ ^[7,12-16] and a Bi coverage of two-thirds ML, the honeycomb phase is achieved. These three phases of bismuth on the Si(111) 7×7 surface exhibit the same reconstruction, presenting the $\sqrt{3} \times \sqrt{3}R30^\circ$, for short, later called $\sqrt{3} \times \sqrt{3}$ -Bi, to which different structural models correspond^[7,17-21].

In the case of α -phase Bi (i.e., a coverage of one-third at high temperature), numerous structural atomic configurations were explored: the so-called T_1 , T_4 , H_3 , and S_3 models. The T_1 configuration allocates the atoms of Bi above the atoms of Si, which belong to the first layer, leaving active two dangling bonds of silicon; indeed, in the T_4 and H_3 configurations, there is a threefold coordination with the Si atoms lying on the first layer, being sitting respectively on top of the Si atoms from the second and fourth layers of the substrate. Furthermore, in the S_3 model, the Bi atoms substitute the ones of the second Si layer, which are positioned at the T_4 sites. The T_4 model is considered, from the energy minimization point of view, the most probable for this α -phase Bi^[15,16]. Therefore, in this $1/3$ ML T_4 structure, each Bi atom, sitting above the second layer of the silicon surface atoms, binds with three surface atoms, completely filling the p shell, saturating the surface dangling bonds, and thus passivating the surface^[12,15,16].

In the β -phase (1 ML), the structural model is named milkstool due to its peculiar structural shape, where the Bi atoms form trimers, being sideways shifted from the T_1 sites, whose centers sit above the T_4 site. Thus, the Si atoms from the substrate, rather than carrying one dangling bond, bind to one Bi adatom; Bi then shares electrons with the two nearest-neighbors Bi adatoms, thereby forming the trimer structure^[3,10-12].

In the third phase, the $2/3$ ML honeycomb structure^[11,17], which appears to show a hexagonal structure, the atoms of bismuth are placed on T_1 sites, right above the atoms of silicon of the upper layer. One-third of the dangling bonds of the substrate are left unsaturated, making it, more properly, a metastable phase.

Without going into too much detail, we would like to mention the physical importance of the interfaces formed with Bi atoms, in which a two-dimensional (2D) system, such as a surface or interface, can give rise to a spin-polarized 2D electron structure, originating from a structural inversion asymmetry and spin-orbit coupling interaction, formed even on nonmagnetic materials. This effect is called Rashba-Bychkov (RB)^[22], and it is the key ingredient in spintronics. This RB effect was observed both on the clean surface of noble metal^[23] and on the heavy element of the V group^[24], as well as on Bi/Ag(111), where giant spin-splitting appeared through surface alloying of heavy metal atoms adsorbed on a lighter substrate^[25]. Even more, a similar behavior could be expected on the interface formation between Bi and much lighter Si atoms.

Particularly intriguing is the case of a one-atom-thick layer of bismuth, organized in a honeycomb grating, called bismuthene, obtained on the insulating silicon carbide substrate, SiC(0001). It has been considered as a structure promoted to exhibit high-temperature quantum spin-Hall effect, as shown by scanning tunneling spectroscopy (STS), which, amazingly enough, depicts a wide gap of ~ 0.8 eV, with conductive edge states^[26].

Equally interesting is the silicene system, a honeycomb layer of one layer of Si atoms, buckled^[27] or flat^[28], or an ensemble of stacks of silicene layers, called multilayer silicene^[29-36].

In particular, recently, silicene and multilayer silicene have been experimentally realized on the α -phase $\sqrt{3} \times \sqrt{3}R30^\circ$ -Bi on Si(111) 7×7 surface used as a template, and supported by first-principles theoretical calculations^[37].

This work focuses on the formation and investigation of the structural and electronic properties of 2D Si(111) islands on β -phase $\sqrt{3} \times \sqrt{3}R30^\circ$ -Bi on Si(111) 7×7 surface, through low energy electron diffraction (LEED), reflection high electron energy diffraction (RHEED), Auger electron spectroscopy (AES), grazing incidence X-ray diffraction (GIXRD), scanning tunneling microscopy (STM), and STS. Furthermore, the band gap of the Si islands on β -phase Si(111) $\sqrt{3} \times \sqrt{3}R30^\circ$ -Bi has been explored by STS, which was determined to be ~ 0.55 eV, exhibiting great potential for various electronic and optoelectronic applications, providing additional insights into the microstructures of silicon.

MATERIALS AND METHODS

The research was executed both at the Institute of Structure of Matter laboratories by Tor-Vergata Campus (Rome, Italy), National Research Council, and at the Institute of Physics by Maria Curie-Skłodowska University (Lublin, Poland). AES spectra were collected using an electron beam energy $E = 2.5$ keV, setting the electron energy analyzer, a double-pass cylindrical mirror PHY 255G, acquisition mode in the first derivative, at an energy resolution of about 0.5 eV. In order to reconstruct the surface of Si(111), the substrates were annealed by applying several flash cycles at approximately 1,423 K, at the beginning for a few seconds and at the end for 60 s, in an ultra-high vacuum (UHV) apparatus, having a base pressure of about 4×10^{-11} mbar. Bi (99.999%, MATEK Material Technologie Kristalle GmbH) was evaporated on Si(111) (p-doped, 2.5 ohm-cm CZ wafer, MEMC Electronic Material S.p.A.) kept at ~ 523 K at a rate of ~ 0.02 ML/min from a Bi solid source, at a Bi pressure of about 4×10^{-8} mbar, up to ~ 1 ML, in order to form the β -phase of Si(111) $\sqrt{3} \times \sqrt{3}R30^\circ$ -Bi, hereafter called Si(111) $\sqrt{3} \times \sqrt{3}$ -Bi. Silicon was evaporated by means of a solid source after the formation of this interface, kept at ~ 473 K, using a low flux rate of about 0.01 ML/min, at a Si pressure of about 4×10^{-10} mbar, and up to ~ 1 and ~ 4 MLs. Sharp LEED patterns related to the Si(111) 7×7 , $\sqrt{3} \times \sqrt{3}$ -Bi, and $\sqrt{3} \times \sqrt{3}$ -Si reconstructions were detected. A Panalytical Empyrean diffractometer, in Bragg-Brentano geometry and Cu anode (40 kV, 40 mA), was used to perform XRD measurements, both out- and in-plane. A small angle of tilt ψ offset of 2° was applied to the sample to reach, moving in the grazing incidence, a more surface-sensitive configuration.

STM imaging in constant current topography and STS measurements were carried at room temperature (RT) in UHV systems, with base pressures better than 5×10^{-11} mbar, equipped with an Omicron LT-STM, RHEED apparatus, and Bi and Si sources. An n-type doped Si(111) sample, with low resistance of $0.003 \Omega\cdot\text{cm}$ at RT, was used in the experiments.

All samples were cleaned in UHV by applying several flashes up to about 1,200 °C from a few seconds up to tens of seconds. Next, ~ 1.2 ML Bi [counted as $\frac{1}{2}$ Si(111) bilayer atom density] was deposited at RT. The β -phase of Si(111) $\sqrt{3} \times \sqrt{3}R30^\circ$ -Bi surface reconstruction was achieved by post-annealing with direct current heating of the sample up to ~ 523 K. The appearance of the $\sqrt{3} \times \sqrt{3}$ reconstruction upon heating current and/or annealing time was easily detected by RHEED. Then, ~ 0.27 ML of Si was deposited onto β -phase Bi on Si(111), keeping the substrate at ~ 493 K (rate of 1 ML / 60 min). The deposition rate was controlled with a quartz crystal microbalance.

RESULTS AND DISCUSSION

Figure 1A illustrates the characteristic diffraction pattern related to the 7×7 of the Si(111) reconstructed surface. The 1×1 unit cell of the unreconstructed Si(111) is characterized by a red rhombus, while the

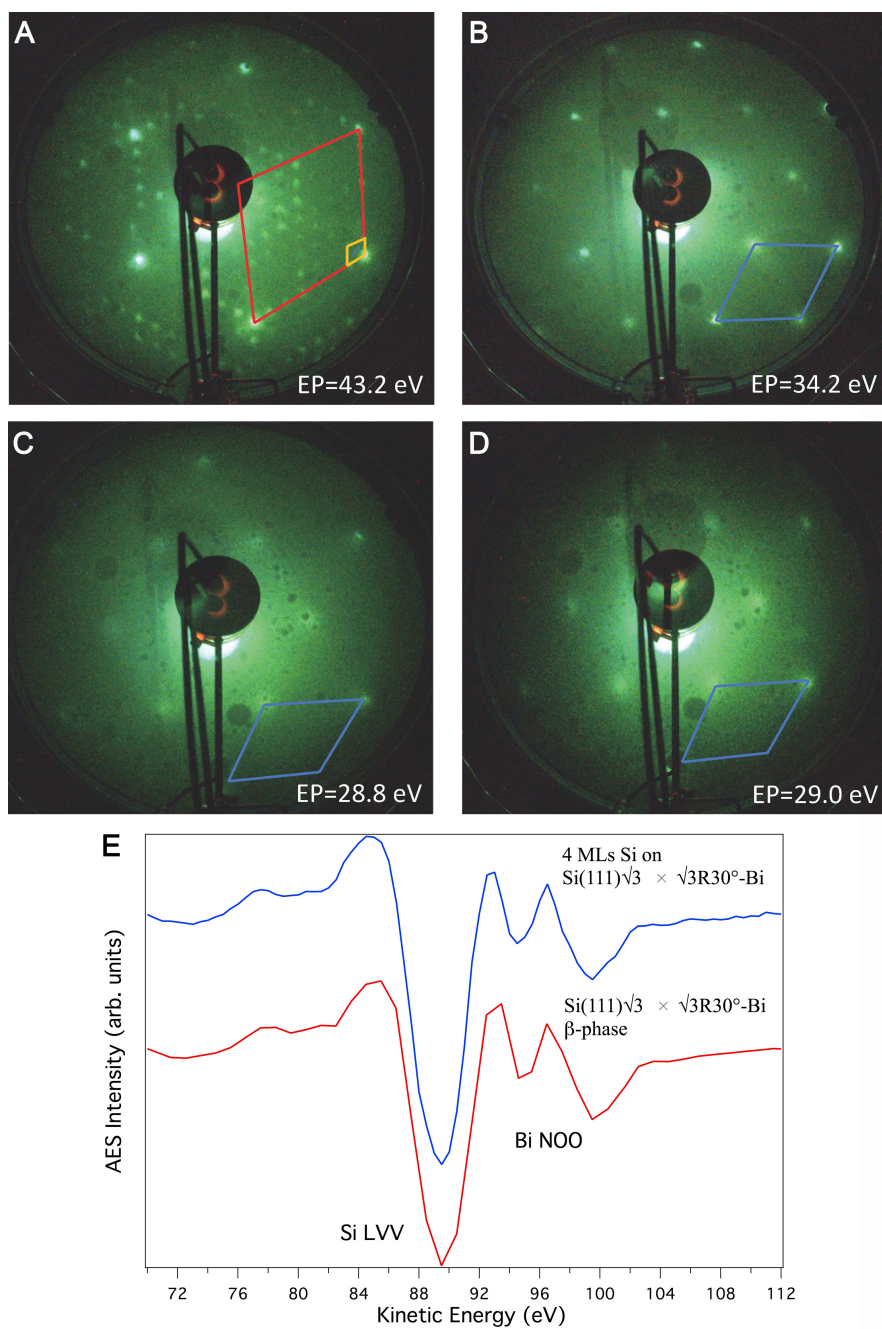


Figure 1. LEED Patterns and AES spectrum are reported in (A-E). (A) LEED pattern from: $\text{Si}(111)7 \times 7$; (B) LEED pattern from $\text{Si}(111)\sqrt{3} \times \sqrt{3}R30^\circ\text{-Bi}$ β -phase; (C) LEED pattern from 1 ML Si / $\text{Si}(111)\sqrt{3} \times \sqrt{3}R30^\circ\text{-Bi}$; (D) LEED pattern from 4 MLs Si / $\text{Si}(111)\sqrt{3} \times \sqrt{3}R30^\circ\text{-Bi}$. The red rhombus in (A) indicates the (1×1) unit cell of $\text{Si}(111)$, while the yellow one indicates the 7×7 -Si surface reconstruction. The blue unit cell in (B-D) represents the $\sqrt{3} \times \sqrt{3}R30^\circ$ of Bi on Si and that of 1 and 4 MLs of silicon grown on top of bismuth. The LEED patterns were collected at primary energy, EP, of 43.2, 34.2, 28.8, and 29.0 eV, respectively; (E) AES from $\text{Si}(111)\sqrt{3} \times \sqrt{3}R30^\circ\text{-Bi}$ β -phase, and 4 MLs Si/ $\text{Si}(111)\sqrt{3} \times \sqrt{3}R30^\circ\text{-Bi}$ interface. The Si LVV and Bi NOO Auger transitions are marked. LEED: Low energy electron diffraction; AES: Auger electron spectroscopy; ML: monolayer.

smaller cell, marked by the yellow rhombus, is the one of the $\text{Si}(111)7 \times 7$ reconstruction. After the formation of the β -phase of 1 ML of $\sqrt{3} \times \sqrt{3}\text{-Bi}$ on $\text{Si}(111)$, the LEED pattern reported in [Figure 1B](#) shows the complete disappearance of the $\text{Si}(111)7 \times 7$ reconstruction. The occurrence of the new $\sqrt{3} \times \sqrt{3}$

reconstruction related to bismuth, marked by the blue rhombus, rotated by 30° with respect to that of the unreconstructed silicon, is clearly visible. This $\sqrt{3} \times \sqrt{3}$ reconstruction is maintained for both 1 and 4 MLs of Si deposited in this β -phase of Bi, as evidenced by the LEED patterns of [Figure 1C](#) and [D](#). [Figure 1E](#) is characteristic of the Si LVV and Bi NOO Auger transitions, located at 91 and 101 eV, respectively, measured from 4 MLs Si grown on top of β -phase of Bi/Si interface, and, for comparison, $\text{Si}(111)\sqrt{3} \times \sqrt{3}R30^\circ$ -Bi β -phase, denoting an increasing of Si LVV signal with respect to Bi NOO, after the Si deposition.

The Si substrate was kept at a temperature of about ~ 473 K, and the unit cells of these Si growths, represented in [Figure 1C](#) and [D](#) also by blue rhombuses, as a guide for the eyes, are overlapped and rotated 30° with respect to that of the $\text{Si}(111)7 \times 7$. In these LEED patterns, the background is faintly increased, compared to the interface of bismuth on silicon, as well as the LEED spots, appearing pale and rather broad.

Although unusual, the $\sqrt{3} \times \sqrt{3}$ reconstruction of bare silicon can take place on the surface of clean $\text{Si}(111)$, as already observed in the past^[38,39]. In this context, this occurrence is particularly interesting since it constitutes a term of comparison with what was obtained for the synthesized multilayer silicene, instead on the β -phase of Bi interface on $\text{Si}(111)$ ^[37].

[Figure 2A](#) shows the XRD measurements acquired on 4 MLs of silicon deposited on the $\sqrt{3} \times \sqrt{3}$ β -phase of the interface of Bi/Si(111), while [Figure 2B](#) is the draft of the used XRD experimental setup.

XRD pattern of [Figure 2A](#) was collected slightly out of plane after performing a rocking curve to reduce the contribution of the Si substrate and detect, eventually, a newly appearing peak ($\alpha = 1.50^\circ$). The tilting of the sample along the α -direction preserves the whole X-ray in-plane scattering angle and, therefore, the position of the XRD reflections, reducing the signal belonging to the monocrystalline silicon substrate, allowing us to probe the contribution from the Si film. Here, we can observe that only a broad XRD peak is present at an angle of $2\theta = 28.445^\circ$ (2). This peak comprises both the $\text{Si}(111)$ substrate and Si film, where the full width at half maximum is $0.160^\circ \pm 0.005^\circ$. It is attributed to the (111) reflection of the [111] planes of the silicon substrate, overlapped with the stacked layers of the Si film. By simply applying the law of Bragg ($2d = n\lambda \sin\theta$, where λ is the incident radiation, $K_\alpha^{\text{Cu}} = 1.540$ Å, and $n = 1$ is the order of the reflection), it was found, for both Si substrate and film, $d_{\text{Si}(111)} = 3.140$ Å (5), in close agreement with the values achieved in^[33-36] for Si substrate alone.

The insert of [Figure 2A](#) reports the GIXRD pattern collected from 4 MLs of Si on the β -phase $\text{Si}(111)\sqrt{3} \times \sqrt{3}$ -Bi interface at $\alpha = 1.50^\circ$, and $\psi = 2.0^\circ$ offset out of the plane. The distance of in-plane lattice parameters for the $\text{Si}(111)\sqrt{3} \times \sqrt{3}$ substrate, obtained after the Bi/Si(111) interface formation, is maintained after 4 MLs of Si deposition film. This gives a unique overlapped unit $\sqrt{3} \times \sqrt{3}$ mesh for the GIXRD Si film peak parallel to $\sqrt{3} \times \sqrt{3}$ Bi/Si(111) interface, showing a distance of $d = 6.61$ (3) Å, in agreement with LEED patterns. This demonstrates that the Si film is formed by stacked layers of tetragonal Si, and not silicene, as recently reported for the Si growth on the $\sqrt{3} \times \sqrt{3}$ α -phase Bi formed on $\text{Si}(111)$ ^[37] and in good agreement with DTF calculations^[40].

[Figure 3A](#) displays a large-scale STM topographic image, (71.5×70.2) nm², recorded on ~ 0.27 ML Si deposited at ~ 220 °C on $\text{Si}(111)\sqrt{3} \times \sqrt{3}$ -Bi β -phase interface. The corresponding height profile traced in [Figure 3A](#) is reported in [Figure 3B](#), in addition to four colored arrows, set in order to better highlight some main interesting sites on the surface.

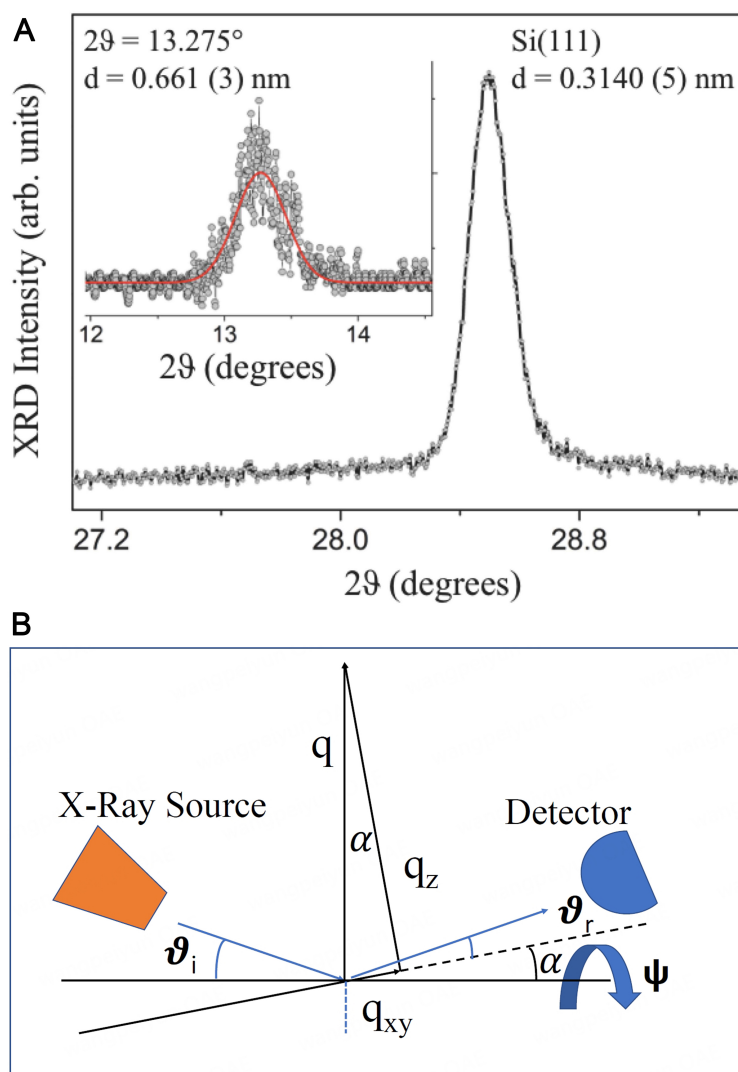


Figure 2. XRD spectrum and the XRD experimental setup are shown in (A) and (B). (A) XRD from 4 MLs of silicon deposited on the $\sqrt{3} \times \sqrt{3}$ β -phase of Bi/Si(111) interface; (B) sketch of the XRD experimental setup, allowing the momentum transfer to be sensitive to the film surface structure at $\vartheta_i = \vartheta_r$, being ϑ_i and ϑ_r the incident and reflected scattering angles; α is the in-plane tilt; while ψ is the out of plane tilt. The insert in (A) is the GIXRD spectrum with $\alpha = 1.50^\circ$ and $\psi = 2.0^\circ$. The GIXRD pattern collected from 4 MLs of Si on the β -phase Si(111) $\sqrt{3} \times \sqrt{3}$ -Bi interface at $\alpha = 1.50^\circ$, and $\psi = 2.0^\circ$ offset out of the plane is presented in the inset of (A). XRD: X-ray diffraction; ML: monolayer; GIXRD: grazing incidence X-ray diffraction.

At a first visual inspection, it can be observed that the STM image shows several defined silicon islands on top of the substrate. They are iso-distributed on both large terraces, appearing brighter on the left and darker on the right. Most of these Si islands have diameters between 3 and 5 nm. Some of them are especially regular, exhibiting a very flat surface. All of this is shown in the profile of [Figure 3B](#), where a line has been drawn on both the silicon islands of the upper terrace and those of the lower one, intersecting the substrate terrace step. The colored triangles mark the sites where the profile heights were calculated, reporting for the blue one an average island height of 0.32 ± 0.03 nm, a value also found on the height of the island of the lower terrace, whereas the Si(111) step height, marked with two red triangles in [Figure 3B](#), is 0.33 ± 0.03 nm high, in good agreement with the atomic step of Si(111)^[41].

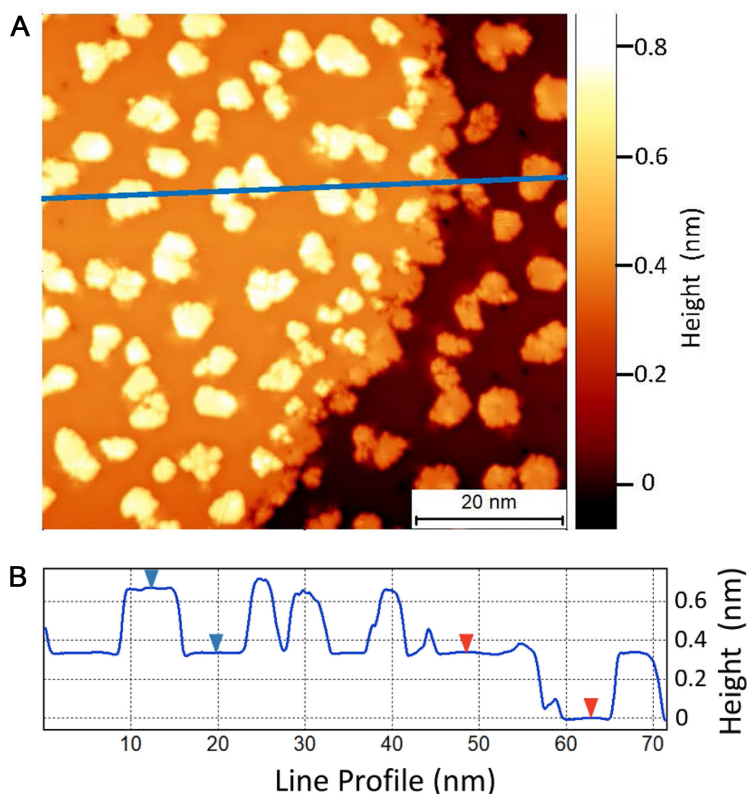


Figure 3. The filled-states STM image and height profile are presented in (A) and (B). (A) STM image (71.5×70.2 nm²) with a sample bias of -3.0 V and tunneling current $I = 100$ pA from -0.27 ML of Si deposited at -220 °C on Si(111) $\sqrt{3} \times \sqrt{3}$ -Bi β -phase; (B) height profile along the line marked in Figure 1A. In Figure 1B, the positions of blue and red triangles were used to determine the height of the Si island and the step height of the Si(111) substrate with $\sqrt{3} \times \sqrt{3}$ -Bi β -phase, respectively. STM: Scanning tunneling microscopy; ML: monolayer.

To highlight the atomic structure of both Si islands and Bi/Si(111) interface, the high-resolution (HR) empty-states STM images, (14.3×14.0 nm²), are shown in Figure 4A and B, where Figure 4A represents the raw data, and Figure 4B those filtered with the fast Fourier transform (FFT), mediated by a broad band pass filter.

The Si islands and Bi/Si(111) in Figure 4A are labeled. It should be noted that all Si islands are commensurate with the Si(111) substrate, as shown by the main crystallographic directions $[\bar{2}11]$, $[\bar{1}2\bar{1}]$ and $[\bar{1}\bar{1}2]$ of Si islands and of the Bi-passivated Si(111) surface. They are marked by continuous lines, which include the $\sqrt{3} \times \sqrt{3}$ superstructure of the substrate and Si islands, clearly visible on both images. The lattice unit length determined from these images is 0.68 ± 0.04 nm.

However, the reconstruction pattern in the Si islands is shifted with respect to the Bi/Si(111) direction, and this shift can vary from island to island [Figure 4B], by the two parallel lines along the $[\bar{2}11]$ direction. Apparently, the existence of several energetically equivalent adsorption sites for Si could be possible, producing, in all the 2D Si islands, the same compelled $\sqrt{3} \times \sqrt{3}$ reconstruction. Such a scenario was recently, albeit for Si on α -phase bismuth-passivated Si surface, theoretically predicted^[40] where three types of silicene adsorption sites were found.

Although the surface reconstruction of Bi/Si(111) shown in Figure 4 appears similar to that of the typical Si(111) $\sqrt{3} \times \sqrt{3}$ -Bi α -phase, it is, instead, the Bi β -phase, whose STM images strongly depend on the applied

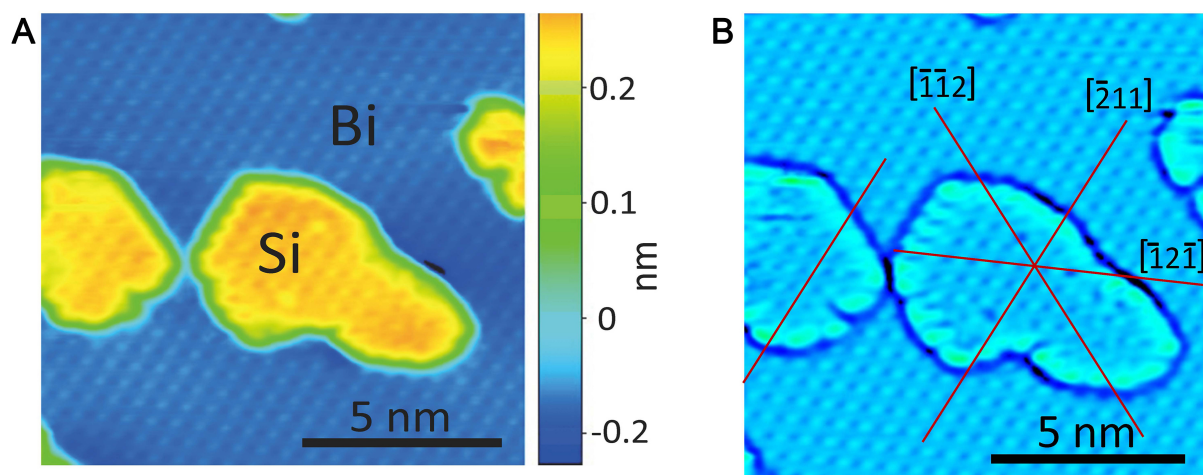


Figure 4. The empty-states STM images are reported in (A) and (B). (A) raw data STM image at a sample bias of +1.7 V and tunneling current $I = 500$ pA (14.3×14.0) nm² from ~ 0.27 ML of Si deposited at ~ 220 °C on Si(111) $\sqrt{3} \times \sqrt{3}$ -Bi β -phase; (B) slight FFT filtering of (A) using broad band pass filter. The Si islands and Bi/Si(111) in (B) are labeled, as well as the main crystallographic directions $[\bar{2}11]$, $[\bar{1}2\bar{1}]$ and $[\bar{1}\bar{1}2]$ of Si and the Bi/Si(111) interface, indicated by continuous lines, and including the $\sqrt{3} \times \sqrt{3}$ surface reconstructions. STM: Scanning tunneling microscopy; ML: monolayer; FFT: fast Fourier transform.

tunneling bias^[20].

This behavior is shown in Figure 5A, where the HR filled-states STM image (2.86×2.81) nm² at reversed voltage with respect to that of Figure 4A and B, bias voltage equal to -1.7 V and tunneling current $I = 100$ pA, clearly evidence the trimers arrangement of Si(111) $\sqrt{3} \times \sqrt{3}$ -Bi β -phase^[2,3,20,40]. The line profile traced in Figure 5A is reported in Figure 5B. This height profile evidences, indeed, that the lattice parameter of Si(111) $\sqrt{3} \times \sqrt{3}$ -Bi β -phase surface reconstruction is 0.67 nm, perfectly in agreement with that of surface reconstruction Si islands- $\sqrt{3} \times \sqrt{3}$, whose value is 0.668 nm, and the results derived from XRD and GIXRD.

The $I(V)$ measurements performed on the Si(111) $\sqrt{3} \times \sqrt{3}$ -Bi β -phase and Si island- $\sqrt{3} \times \sqrt{3}$ surface reconstruction are reported in Figure 6.

Both islands and substrate show semiconducting character with an energy gap of around 0.5 eV. We have validated some scattered data of energy gaps not only for different islands but also within a certain island. Therefore, the value of 0.5 eV bears some uncertainty of about ± 0.2 eV. On the contrary to what is expected for nanostructures, where quantum size effect usually produces a wider band gap^[42], in our 2D Si islands, a reduced band gap has been observed. This evidence finds a possible explanation in a Si doping effect due to the underneath Bi layer in the Si/Bi interface formation. On the other hand, two observations have to be taken into consideration: the first is that, nevertheless, the gaps of A (Bi/Si), 0.59 eV, and B (Si/Bi), 0.55 eV, are not so far very different in value, they are different, manifesting without any doubt, the signature of the two regions. Secondly, being the two interfaces one the opposite of the other, and the Bi layer confined between the Si bulk, and the more surface sensitive 2D Si, an imbalance of the electron doping process could favor the B side (Si/Bi), closing the gap and lacking a true crystalline potential here.

On the contrary, the existence of an energy gap larger than 1 eV was recently determined from STS data on the Si(111) $\sqrt{3} \times \sqrt{3}$ -Bi β -phase interface^[20].

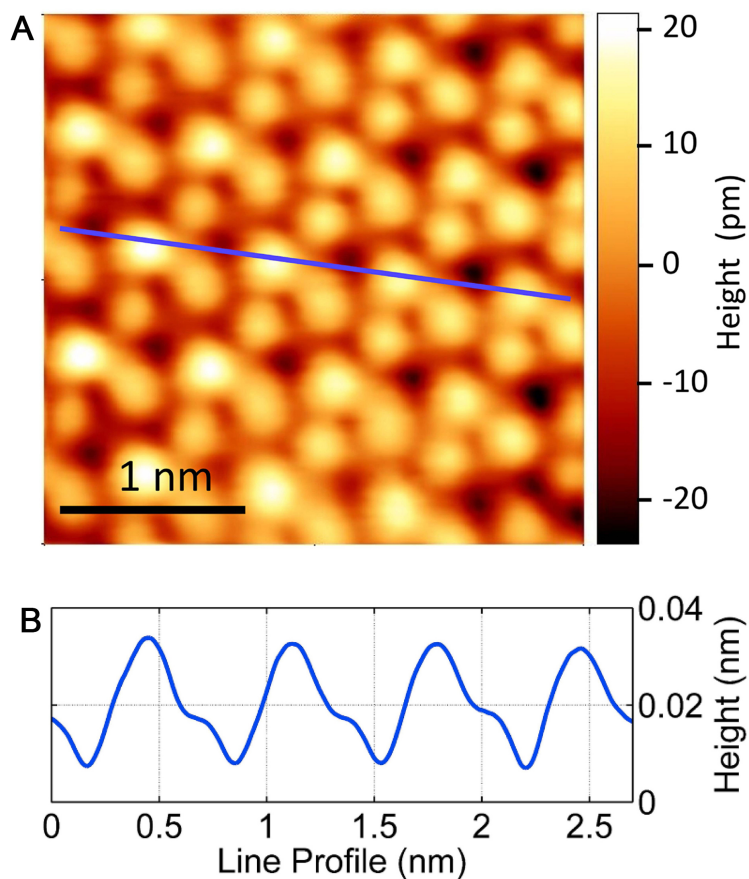


Figure 5. The HR filled-states STM image and height profile are displayed in (A) and (B). (A) STM image (2.86×2.81) nm² collected on Si(111) $\sqrt{3} \times \sqrt{3}$ -Bi β -phase. The image was acquired at -1.7 V bias and tunneling current $I = 100$ pA; (B) height profile along the line marked in (A). HR: High-resolution; STM: scanning tunneling microscopy.

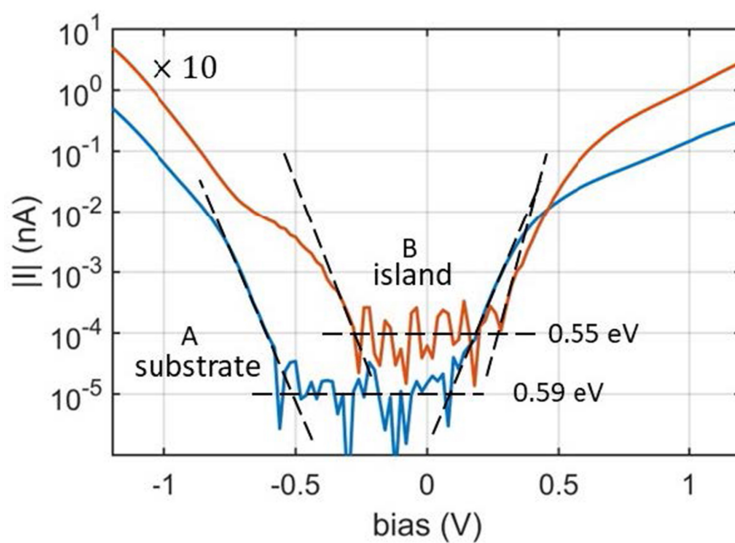


Figure 6. I-V characteristics are reported in this figure; the blue curve, A, is collected in the surface reconstruction Si(111) $\sqrt{3} \times \sqrt{3}$ -Bi β -phase, and the brown curve, B, in Si island- $\sqrt{3} \times \sqrt{3}$. For better visibility, curve B is multiplied tenfold. The dashed lines illustrate the methodology for determining the energy gap. Note that the tunneling current signal span spans almost five decades. The energy gaps are determined at a measured current level of 10 fA, which is the average noise of the current-voltage converter.

A possible understandable disagreement between STS data of Ref.^[20] and data reported in [Figure 6](#) might be due to a different method of presentation. One has to be aware of very strong dependence of the tunneling current versus tunneling bias, when electron density falls rapidly toward Fermi energy for semiconductors with surface states within the gap. According to density functional theory (DFT) calculations, such states are present in the Ref.^[20]. Therefore, a good method to explore states within an energy gap is to determine biases when the tunneling current approaches the unavoidable noise of the tunneling current preamplifier. This determines the limit of the given tunneling microscope. Indeed, the shape of the left side of curve B in [Figure 6](#) clearly deviates from the right side, indicating the presence of additional states at the edge of the valence band. This is in perfect agreement with DFT calculations of Ref.^[20] [[Figure 2A](#)] showing projected density of states results for Bi surface states in Si(111) $\sqrt{3} \times \sqrt{3}$ -Bi. Moreover, the tunneling curve B for the Si island compared to the A curve for the substrate is shifted by about 0.18 eV towards higher energy, indicating depletion of the surface states on the island in favor of substrate charging.

CONCLUSIONS

Si films were grown in UHV after the $\sqrt{3} \times \sqrt{3}R30^\circ$ interface formation of the β -phase of bismuth on the Si(111) 7×7 surface reconstruction. LEED, AES, XRD, GIXRD, STM, and STS have been used for the investigation of the Bi/Si(111) interface and Si film growth. Si islands with $\sqrt{3} \times \sqrt{3}$ reconstruction, commensurate with Bi/Si(111), have been found. All reported results point to the synthesis of (111) stacked Si layers, with a Si-Si along the (111) planes of about $d_{\text{Si}(111)} = 3.140 \text{ \AA}$ (5). This constitutes an interesting example of surface science involving 2D materials, where the same reconstruction, $\sqrt{3} \times \sqrt{3}$, same elements, Bi and Si, same substrate, Si(111), give rise to different Si growth, silicene, in the case of the Si(111) $\sqrt{3} \times \sqrt{3}$ -Bi α -phase, and 2D Si(111) islands on the Si(111) $\sqrt{3} \times \sqrt{3}$ -Bi β -phase^[37,40], with a decreased band gap, with respect to the ordinary Si(111), due to the presence of the beneath Bi layer.

DECLARATIONS

Acknowledgments

The authors would like to thank Sandro Priori, Alessandro Ippoliti, and Marco Guaragno for their invaluable technical help.

Authors' contributions

Conceptualization: De Padova P, Krawiec M

Formal analysis: De Padova P, Ottaviani C, Quaresima C, Generosi A, Paci B, Olivieri B, Jałochowski M, Krawiec M

Funding acquisition: De Padova P, Krawiec M

Investigation: De Padova P, Ottaviani C, Quaresima C, Generosi A, Paci B, Olivieri B, Jałochowski M, Krawiec M

Project administration: De Padova P, Krawiec M

Writing-original draft: De Padova P

Writing-review and editing: De Padova P, Ottaviani C, Quaresima C, Generosi A, Paci B, Olivieri B, Jałochowski M, Krawiec M

All authors have read and agreed to the published version of the manuscript.

Availability of data and materials

Not applicable.

Financial support and sponsorship

This work was supported by the National Science Centre, Poland, under grant no. 2018/29/B/ST5/01572 and Vth Committee of INFN within the NUCLEAAR Project.

Conflicts of interest

All authors declared that there are no conflicts of interest.

Ethical approval and consent to participate

Not applicable.

Consent for publication

Not applicable.

Copyright

© The Author(s) 2024.

REFERENCES

1. Mohan R. Green bismuth. *Nat Chem* 2010;2:336. [DOI](#) [PubMed](#)
2. Takahashi T, Izumi K, Ishikawa T, Kikuta S. Evidence for a trimer in the $\sqrt{3} \times \sqrt{3}$ -Bi structure on the Si(111) surface by X-ray diffraction under the nearly normal incidence condition. *Surf Sci Lett* 1987;183:L302-12. [DOI](#)
3. Takahashi T, Nakatani S, Ishikawa T, Kikuta S. Surface structure analysis of Si(111) $\sqrt{3} \times \sqrt{3}$ -Bi by X-ray diffraction - Approach to the solution of the phase problem. *Surf Sci Lett* 1987;191:L825-34. [DOI](#)
4. Park CY, Abukawa T, Higashiyama K, Kono S. Analysis of the atomic structure of the Si(111) $\sqrt{3} \times \sqrt{3}$ -Bi surface by X-ray photoelectron diffraction. *Jpn J Appl Phys* 1987;26:L1335. [DOI](#)
5. Shioda R, Kawazu A, Baski AA, Quate CF, Nogami J. Bi on Si(111): two phases of the $\sqrt{3} \times \sqrt{3}$ surface reconstruction. *Phys Rev B* 1993;48:4895-8. [DOI](#) [PubMed](#)
6. Park C, Bakhtizin RZ, Tomihiro Hashizume TH, Toshio Sakurai TS. Scanning tunneling microscopy of $\sqrt{3} \times \sqrt{3}$ -Bi reconstruction on the Si(111) surface. *Jpn J Appl Phys* 1993;32:L290. [DOI](#)
7. Park C, Bakhtizin RZ, Tomihiro Hashizume TH, Toshio Sakurai TS. Structure of the Bi/Si(111) surface by field-ion scanning tunneling microscopy. *Jpn J Appl Phys* 1993;32:1416. [DOI](#)
8. Bakhtizin RZ, Park C, Hashizume T, Sakurai T. Atomic structure of Bi on the Si(111) surface. *J Vac Sci Technol B* 1994;12:2052-4. [DOI](#)
9. Roesler JM, Sieger MT, Miller T, Chiang TC. New experimental technique of photoelectron holography applied to Bi trimers on Si(111). *Surf Sci* 1997;380:L485-90. [DOI](#)
10. Cheng C, Kunc K. Structure and stability of Bi layers on Si(111) and Ge(111) surfaces. *Phys Rev B* 1997;56:10283-8. [DOI](#)
11. Roesler JM, Miller T, Chiang TC. Photoelectron holography studies of Bi on Si(111). *Surf Sci* 1998;417:L1143-7. [DOI](#)
12. Nakatani S, Takahashi T, Kuwahara Y, Aono M. Use of x-ray reflectivity for determining the Si(111) $\sqrt{3} \times \sqrt{3}$ -Bi surface structures. *Phys Rev B* 1995;52:R8711-4. [DOI](#)
13. Miwa RH, Schmidt TM, Srivastava GP. Bi covered Si(111) surface revisited. *J Phys Condens Matter* 2003;15:2441. [DOI](#)
14. Yaginuma S, Nagao T, Sadowski JT, et al. Origin of flat morphology and high crystallinity of ultrathin bismuth films. *Surf Sci* 2007;601:3593-600. [DOI](#)
15. Wan KJ, Guo T, Ford WK, Hermanson JC. Initial growth of Bi films on a Si(111) substrate: two phases of $\sqrt{3} \times \sqrt{3}$ low-energy-electron-diffraction pattern and their geometric structures. *Phys Rev B* 1991;44:3471-4. [DOI](#) [PubMed](#)
16. Wan KJ, Guo T, Ford WK, Hermanson JC. Low-energy electron diffraction studies of Si(111)-($\sqrt{3} \times \sqrt{3}$)R30°-Bi system: observation and structural determination of two phases. *Surf Sci* 1992;261:69-87. [DOI](#)
17. Woicik JC, Franklin GE, Liu C, et al. Structural determination of the Si(111) $\sqrt{3} \times \sqrt{3}$ -Bi surface by x-ray standing waves and scanning tunneling microscopy. *Phys Rev B* 1994;50:12246-9. [DOI](#)
18. Kuzumaki T, Shirasawa T, Mizuno S, Ueno N, Tochihiro H, Sakamoto K. Re-investigation of the Bi-induced Si(111)-($\sqrt{3} \times \sqrt{3}$) surfaces by low-energy electron diffraction. *Surf Sci* 2010;604:1044-8. [DOI](#)
19. Berntsen MH, Götberg O, Tjernberg O. Reinvestigation of the giant Rashba-split states on Bi-covered Si(111). *Phys Rev B* 2018;97:125148. [DOI](#)
20. Chi L, Nogami J, Singh CV. Bias dependence and defect analysis of Bi on Si(111) $\sqrt{3} \times \sqrt{3}$ β -phase. *Phys Rev B* 2021;103:075405. [DOI](#)
21. Hsieh SC, Hsu CH, Chen HD, Lin DS, Chuang FC, Hsu PJ. Extended α -phase Bi atomic layer on Si(111) fabricated by thermal desorption. *Appl Surf Sci* 2020;504:144103. [DOI](#)
22. Bychkov YA, Rashba ÉI. Properties of 2D electron gas with lifted spectral degeneracy. *JETP Lett* 1984;39:78-81. Available from: http://jetpletters.ru/ps/1264/article_19121.pdf. [Last accessed on 7 Apr 2024]
23. LaShell S, McDougall BA, Jensen E. Spin splitting of an Au(111) surface state band observed with angle resolved photoelectron spectroscopy. *Phys Rev Lett* 1996;77:3419-22. [DOI](#) [PubMed](#)
24. Koroteev YM, Bihlmayer G, Gayone JE, et al. Strong spin-orbit splitting on Bi surfaces. *Phys Rev Lett* 2004;93:046403. [DOI](#)

25. Ast CR, Henk J, Ernst A, et al. Giant spin splitting through surface alloying. *Phys Rev Lett* 2007;98:186807. [DOI](#)
26. Reis F, Li G, Dudy L, et al. Bismuthene on a SiC substrate: a candidate for a high-temperature quantum spin Hall material. *Science* 2017;357:287-90. [DOI](#)
27. Vogt P, De Padova P, Quaresima C, et al. Silicene: compelling experimental evidence for graphenelike two-dimensional silicon. *Phys Rev Lett* 2012;108:155501. [DOI](#)
28. Stpniak-dybala A, Dyniec P, Kopciuszyski M, Zdyb R, Jałochowski M, Krawiec M. Planar silicene: a new silicon allotrope epitaxially grown by segregation. *Adv Funct Mater* 2019;29:1906053. [DOI](#)
29. De Padova P, Avila J, Resta A, et al. The quasiparticle band dispersion in epitaxial multilayer silicene. *J Phys Condens Matter* 2013;25:382202. [DOI](#)
30. De Padova P, Vogt P, Resta A, et al. Evidence of Dirac fermions in multilayer silicene. *Appl Phys Lett* 2013;102:163106. [DOI](#)
31. Vogt P, Capiod P, Berthe M, et al. Synthesis and electrical conductivity of multilayer silicene. *Appl Phys Lett* 2014;104:021602. [DOI](#)
32. Grazianetti C, Cinquanta E, Tao L, et al. Silicon nanosheets: crossover between multilayer silicene and diamond-like growth regime. *ACS Nano* 2017;11:3376-82. [DOI](#)
33. De Padova P, Ottaviani C, Quaresima C, et al. 24 h stability of thick multilayer silicene in air. *2D Mater* 2014;1:021003. [DOI](#)
34. De Padova P, Generosi A, Paci B, et al. Multilayer silicene: clear evidence. *2D Mater* 2016;3:031011. [DOI](#)
35. De Padova P, Feng H, Zhuang J, et al. Synthesis of multilayer silicene on Si(111) $\sqrt{3} \times \sqrt{3}$ -Ag. *J Phys Chem C* 2017;121:27182-90. [DOI](#)
36. De Padova P, Generosi A, Paci B, et al. New findings on multilayer silicene on Si(111) $\sqrt{3} \times \sqrt{3}$ R30°-Ag template. *Materials* 2019;12:2258. [DOI PubMed PMC](#)
37. Garagnani D, De Padova P, Ottaviani C, et al. Evidence of sp^2 -like hybridization of silicon valence orbitals in thin and thick Si grown on α -phase Si(111) $\sqrt{3} \times \sqrt{3}$ R30°-Bi. *Materials* 2022;15:1730. [DOI PubMed PMC](#)
38. Berghaus T, Brodde A, Neddermeyer H, Tosch S. STM observation of a new reconstruction on narrow Si(111) terraces. *Surf Sci* 1987;181:340-5. [DOI](#)
39. Fan WC, Ignatiev A, Huang H, Tong SY. Observation and structural determination of $(\sqrt{3} \times \sqrt{3})R30^\circ$ reconstruction of the Si(111) surface. *Phys Rev Lett* 1989;62:1516-9. [DOI](#)
40. Xu YX, Cao XR, Xu LH, Zheng F, Wu SQ, Zhu ZZ. Silicene adsorption on the bismuth-passivated Si(111) $\sqrt{3} \times \sqrt{3}$ surface: a first-principles study. *Mater Chem Phys* 2018;216:8-13. [DOI](#)
41. Becker RS, Golovchenko JA, McRae EG, Swartzentruber BS. Tunneling images of atomic steps on the Si(111) 7×7 surface. *Phys Rev Lett* 1985;55:2028-31. [DOI](#)
42. Mak KF, Lee C, Hone J, Shan J, Heinz TF. Atomically thin MoS₂: a new direct-gap semiconductor. *Phys Rev Lett* 2010;105:136805. [DOI PubMed](#)